RSC Advances

PAPER

View Article Online
View Journal | View Issue

Cite this: *RSC Adv.*, 2022, **12**, 7864

Catalytic behaviour of the Cu(I)/L/TEMPO system for aerobic oxidation of alcohols – a kinetic and predictive model†

Afnan Al-Hunaiti, *[a] Batool Abu-Radaha,[a] Darren Wraith[b] and Timo Repo [c]

Here, we disclose a new copper(I)-Schiff base complex series for selective oxidation of primary alcohols to aldehydes under benign conditions. The catalytic protocol involves 2,2,6,6-tetramethylpiperidine-*N*-oxyl (TEMPO), *N*-methylimidazole (NMI), ambient air, acetonitrile, and room temperature. This system provides a straightforward and rapid pathway to a series of Schiff bases, particularly, the copper(I) complexes bearing the substituted (furan-2-yl)imine bases *N*-(4-fluorophenyl)-1-(furan-2-yl) methanimine (L2) and *N*-(2-fluoro-4-nitrophenyl)-1-(furan-2-yl)methanimine (L4) have shown excellent yields. Both benzylic and aliphatic alcohols were converted to aldehydes selectively with 99% yield (in 1–2 h) and 96% yield (in 16 h). The mechanistic studies *via* kinetic analysis of all components demonstrate that the ligand type plays a key role in reaction rate. The basicity of the ligand increases the electron density of the metal center, which leads to higher oxidation reactivity. The Hammett plot shows that the key step does not involve H-abstraction. Additionally, a generalized additive model (GAM, including random effect) showed that it was possible to correlate reaction composition with catalytic activity, ligand structure, and substrate behavior. This can be developed in the form of a predictive model bearing in mind numerous reactions to be performed or in order to produce a massive data-set of this type of oxidation reaction. The predictive model will act as a useful tool towards understanding the key steps in catalytic oxidation through dimensional optimization while reducing the screening of statistically poor active catalysis.

Received 25th December 2021
Accepted 25th February 2022

DOI: 10.1039/d1ra09359b

rsc.li/rsc-advances

Introduction

Due to the use of aldehydes and carboxylic acids in various applications, a diverse effort to develop efficient, selective and greener oxidation systems using environmentally friendly catalysts, oxidants, and solvents has become a critical drive for catalysis.[1] Thus, aerobic oxidation at ambient temperature is most preferred. Among numerous methods in the literature, copper (Cu) shows prominent activities for aerobic oxidation,.[2–5] Specifically, Cu (I, II) have been employed in the mediation of nitroxyl-radicals; for example, 2,2,6,6-tetramethylpiperidinyl-1-oxyl (TEMPO) in the past few decades.[6–9] Besides that, being inspired by the catalytic chemistry of the copper-containing enzyme, galactose oxidase (GOase), copper complexes have attracted attention as catalysts in alcohol oxidations.[10–14] It has been reported that the Cu(I)/nitroxyl catalyst systems can catalyse the aerobic oxidations of a variety of substrates, including aromatic alcohols, secondary and sterically hindered alcohols as well as even more complex substrates such as polysaccharides.[15,16]

Recently, it was found by Stahl and co-workers[17,18] that NMI acts both as a base and as a ligand during the catalysis. As an additive, it was found that a certain molar ratio of NMI/Cu alongside another bidentate ligand, for example, 2,2′-bipyridine (bpy), gave the best catalytic performance. By carefully considering the catalyst optimization reported by Stahl and co-workers, the Cu/nitroxyl catalyst system using NMI as the only ligand added into the system could lead to moderate yield (68%).[18,19]

A five member ring Schiff base [(*N*-(4-fluorophenyl)-1-(pyroll-2-yl)methanimine] was recently applied and showed a high reactivity for the primary alcohol oxidation. These Schiff bases have a five-ring bearing oxygen which will behaves as a second donor atom in a bidentate ligand.[18,28–31] Therefore, in this work we focused at studying the substitution effect on such ligands, and subsequently highlight the role of chelating nitrogen ligands on the reaction mechanistic understanding *via* kinetic approach. In our studies, Cu^{I} sources (Cu(OTf) and CuBr) were employed for comparison. The correlation between the ligand type and various

[a]*Department of Chemistry, School of Science, The University of Jordan, Amman 11942, Jordan. E-mail: a.alhunaiti@ju.edi.jo*

[b]*School of Public Health and Social Work, Queensland University of Technology, Queensland 4000, Australia*

[c]*Department of Chemistry, Laboratory of Inorganic Chemistry, University of Helsinki, 00014 Helsinki, Finland*

† Electronic supplementary information (ESI) available. See DOI: 10.1039/d1ra09359b

catalytic reaction parameters were also analysed. To minimize the number of trials required to obtain optimum yield, a predictive model relating reactivity of catalytic system (Cu/L/NMI/TEMPO) to its product selectivity was developed. This would shows the usefulness of modelling approach consists not only in their capability to establish an approximate dependence of the performance of a catalytic material on its properties, but also in the possibility to use them for prediction the reactivity for various substrates.

Experimental

Synthesis and oxidation

Chemicals, solvents and starting materials. Chemicals were obtained from Sigma-Aldrich and used without additional purification. The aerobic oxidation reaction occurred at room temperature with ambient air as the oxidant. The reaction was monitored and quantitatively analysed by Gas Chromatography Mass Spectrometry (GC-MS, Varian 2200) with DB-wax-5MS. The temperature of the GC column was set at 50 °C for 1 min and then was increased to 200 °C at a rate of 10 °C min^{-1}.

Ligand synthesis. Ligands were synthesized according to previously reported protocol.[29] Furfural (1 eq.) and substituted anilines (1.1 eq.) were mixed in a 50 mL round bottom flask with MeOH (5 mL). The reaction was stirred at rt for 1 hour. The crude products were filtered out, sometimes recrystalized and ^{1}H, ^{13}C NMR spectra were recorded. All ligands were synthesized similarly.

Data collection and preparation methods. The data set was collected by careful kinetic measurement of the targeted systems. Each experimental data point was characterized by a set of descriptors for the catalyst formulation and for the reaction conditions. In our framework, we proposed a set of 18 descriptors. The logarithm of the reaction rate (denoted as k) was used as a measure of catalytic activity. The entire data set studied can be found in the ESI.† The original data set contains 890 experimental points. This set was filtered such that only reaction mechanisms and pathways of significant component were used.

Procedure for the aerobic oxidation. Catalytic oxidation of 1-octanol to 1-octanal in acetonitrile was conducted at rt: in a vessel of 10 mL, a solution of CuBr (0.25 mmol, 36.2 mg) and ligand 1–10 (0.5 mmol) were added to 5 mL of CH_3CN. Later other components were added to reaction mixture NMI (0.125–0.5 mmol), and TEMPO (0.125–0.25 mmol, 14.9–39.1 mg) and 1-octanol (5 mmol, 651.0 mg) in open air atmosphere. Then the reaction was carried out at 25 °C for 16 hours under vigorously stirring. The products were analysed by GC using the internal standard method. Quantitative analysis of 1-octanal was achieved by establishing their calibration curves with linear equations under optimized conditions, where the internal standard is 1,2-dichlorobenzene. For other substrates, the oxidation reaction was accordingly preformed.

Generalized additive model (GAM)

We undertook an exploratory data analysis to first examine potential relationships and to identify anomalies in the data or experiments conducted. As some of the experiments were only run once for a particular combination of variables, we restricted the available data to include combinations of variables where a number of experiments were performed. After filtering out these cases, for ligand type (L2 and L4): there were only two different types of growth/yield curves of ligand level available for L2 (levels 4 and 5) and one for L4 (level 4); only one value for TEMPO (equal to 5); two different types of alcohol for both ligand types (alcohol equal to Aliph1 and BOH1); three different levels of pressure (0.95, 0.89, 0.50); one temperature level (equal to 21); and two different values for NMI (5 and 10).

For the main results, we used a Generalised Additive Model (GAM) using a beta distribution and logit link to establish associations/predictors of yield growth for ligand type (L2 and L4). Using a beta distribution naturally constrains the predicted yield to be between 0 and 100% (or 0 and 1). These models can effectively and flexibly allow for non-linear relationships between variables, in this case between yield and time.[32] Other explanatory variables for these observed changes in yield over time (growth curves) can also be included in the regression model in different forms including allowing for interaction terms. Based on the data from the experiments, interaction terms for ligand type were only possible for ligand level, alcohol and NMI. Interaction between these potential predictors (as a three-way interaction) was more limited: alcohol has different levels for NMI (only one experiment for Aliph1); and two different levels for ligand level and NMI. Random effects were also included to allow for heterogeneity between observed growth curves present in the data.

Results and discussion

Optimization of reaction conditions

To examine the optimal reaction conditions for the oxidation, 1-octanol was employed as a model substrate for aerobic catalytic oxidation, Scheme 1. The oxidation is highly solvent dependent as shown in Table 1. Among the common solvents, acetonitrile (MeCN) is the most suitable solvent. It does not seem that there is a straight correlation between the reaction progress and both the polarity, and the coordination character of the solvent can be established. In this work acetonitrile was employed as the reaction medium. The use of water in such systems leads to decrease reactivity and catalyst deactivation.

Ligand effect. The ligands used in this study are basic Schiff base. A series of furan-based Schiff base ligands having different substituted patterns on aniline were studied (Scheme 2). The impact of these modified Schiff base ligands on the catalytic activity was studied by oxidizing 1-octanol under ambient air (Fig. 1). The highest yield for the oxidation of 1-

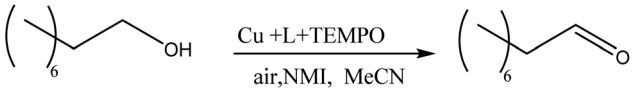

Scheme 1 Cu/TEMPO-based catalytic systems for the aerobic oxidation of primary alcohols.

Table 1 The effect of solvents on the oxidation

Entry	Solvent (3 mL)	Conversion (%)
1	Toluene	5
2	DCM	45
3	MeCN	100
4	Water	18
5	Acetone	15

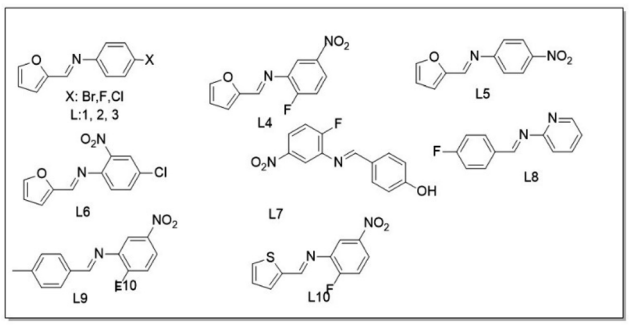

Scheme 2 Representative ligands used in this work.

octanol was obtained by using L2 and L4 as *in situ* made copper complexes ligand. Only modest reactivities were recorded with L6, L7, L8, L9 and L10. Bearing aniline with different substitution the lowest reactivity was observed in L8 (Fig. 1). Although, low steric hindrance is important, these findings indicate that a substituent with a high electronegativity and *para*-directing properties is preferred at the aniline moiety of the ligand. By varying the furan moiety into thiophene, a significant change in catalytic efficiency as indicated in Fig. 1. In the aerobic catalytic oxidation, the activation of O_2 is generally considered an important step and is achieved by its binding to the copper(I) centre. Thus, the electron density on the metal is vital to the catalysis. Basically, the coordination between a metal ion and a ligand is an acid–base reaction, therefore, a ligand with strong

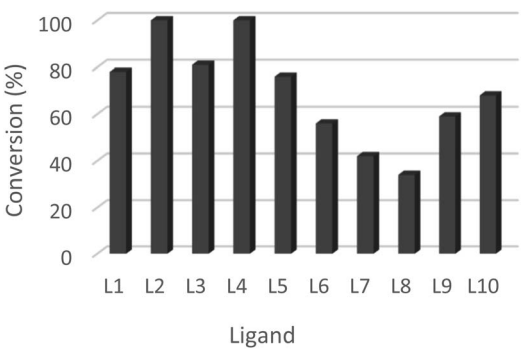

Fig. 1 Ligands efficiency for the oxidation of 1-octanol. Standard reaction conditions: 1-octanol (1 mmol, 130.2 mg), Cu(OTf) (0.05 mmol, 18.8 mg), L (0.05 mmol), TEMPO (0.05 mmol, 14.8 mg), air, 25 °C, 24 h. Conversion calculated by GC analysis using 1,2-dichlorobenzene as internal standard.

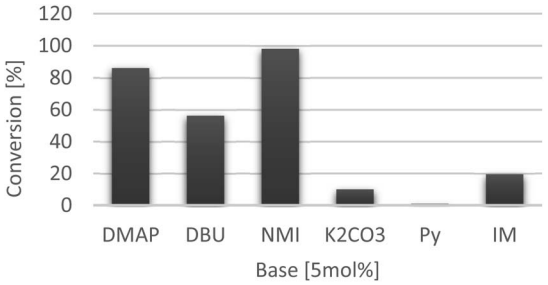

Fig. 2 Base effect on the catalytic reaction using L4. Standard reaction conditions: 1-octanol (1 mmol, 130.2 mg), Cu(OTf) (0.05 mmol, 18.8 mg), TEMPO (0.05 mmol, 14.8 mg), air, 25 °C, 24 h. Conversion calculated by GC analysis using 1,2-dichlorobenzene as internal standard.

basicity can increase the electron density of the metal centre. In this content the ligand L2 and L4 showed higher reactivity.

Base effect. Throughout the investigation, the ligand to metal salt ratio and reaction time were adopted. As the alcohol oxidation involves deprotonation, the base addition may enhance the reaction yield, selectivity and stability of the catalyst. Indeed, various reports have added a base in the catalytic oxidation and shown significant increase in the reaction reactivity.[23–27] Very often, NMI was used as an additive alongside with other bidentate ligands.[27–30] It was believed that NMI acts as a base.[27] However, in the CuI/L4/TEMPO system, other base applied has deteriorated the oxidation reaction, Fig. 2.

Pyridine is good base in numerous reactions, however in our reaction condition it diminish the reaction conversion, possibly due to the coordination with metal salt as ligand, therefore, blocking the chance to the reaction to occur (entry 6, Table 2) whereas inorganic bases are poorly soluble in organic solvents. Therefore, presence of a such base may cause a loss of the reactivity. The low yield can be by forming copper species such Cu(II)-hydroxides which may altering the reaction pathway.[25,27] The observation suggests that either deprotonation is a fast step in the oxidation or there has another pathway involved the need of base in the system, and in this context the NMI has shown the highest reactivity (Fig. 2).

Metal salt effect. In addition to Cu(OTF), a few other Cu(I) salts were also examined (Fig. 3). Both copper bromide and copper triflate (Fig. 3) has excellent catalytic efficiency among all copper salts used (Fig. 3). However, for the cuprous halides, our experiments data suggested, CuBr is practically soluble in acetonitrile whereas the other two are much less soluble in the same solvent which can cause the reactivity variation. Therefore, we have used the cuprous triflate salt when testing the other parameters.

Kinetic studies

Our initial mechanistic studies focused on probing mechanistic differences between two Schiff bases and their effect on the overall mechanism (L2 and L4 Scheme 1). The reaction rate was studied in combination with the other reaction parameters (TEMPO, NMI, alcohol type, copper salts and temperature).

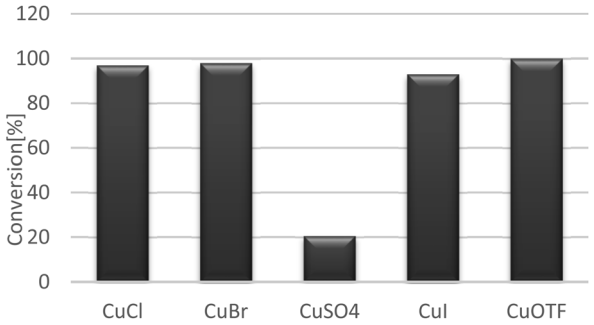

Fig. 3 The catalytic efficiency of various metal (CuI) salts on the aerobic oxidation. Reaction conditions: 1-octanol (1 mmol, 130.2 mg), NMI (0.05 mmol, 8.22 mg), TEMPO (0.05 mmol, 14.8 mg), L4 (0.05 mmol), air, 25 °C, 24 h. Conversion calculated by GC analysis using 1,2-dichlorobenzene as internal standard.

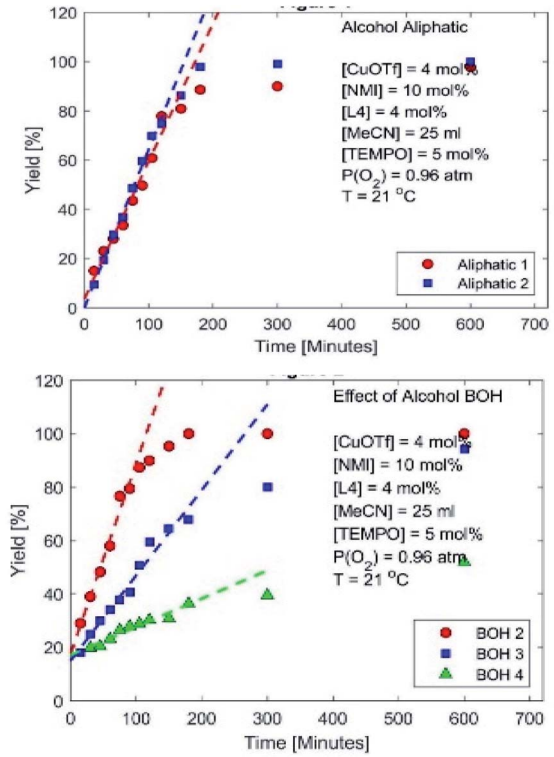

Fig. 4 Time course data for the oxidation of aliphatic (1-octanol, 2-octene-ol), benzyl alcohols (BOH2 benzyl alcohol, BOH3 cinnamyl alcohol, BOH4 diphenylmethanol) using L4.

Table 2 Kinetic dependence for alcohol oxidation using Cu/TEMPO/NMI

	K		*R*	
Parameter	L2	L4		
TEMPO	0.0015	0.0016	0.8990	0.9210
Cu salt	0.0959	0.0204	0.9794	0.9470
O_2	0.0656	0.0945	0.7890	0.6701
NMI	0.0049	0.0050	0.9794	0.9658
Ligand type	0.0832	0.0388	0.8539	0.9585

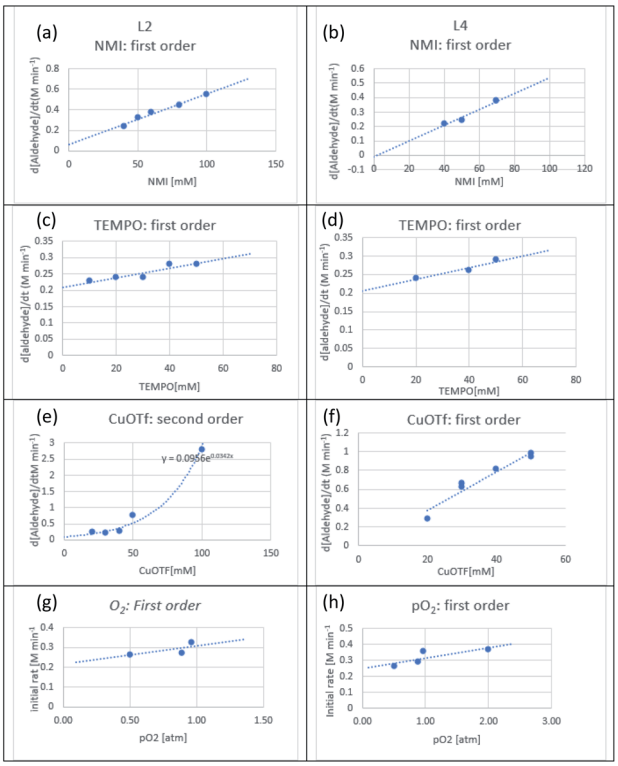

Fig. 5 The kinetic data from oxidation of $PhCH_2OH$ by L/Cu(OTf)/TEMPO assigns the following parameters (a and b) base NMI on L2 and L4, (c and d) TEMPO on L2 and L4, (e and f) CuOTF effect on L2 and L4, and (g and h) O_2 pressure on L2 and L4. Standard reaction conditions: $PhCH_2OH$ (1 mmol, 130.2 mg), Cu(OTf) (0.05 mmol, 18.8 mg), L4 or L4 (0.05 mmol), TEMPO (0.05 mmol, 14.8 mg), air, 25 °C. Conversion calculated by GC analysis using 1,2-dichlorobenzene as internal standard.

First, reaction time plots with different concentrations of aldehyde, determined by GC spectroscopy during the oxidation of benzylic and aliphatic alcohols (Fig. 4). Regarding the benzylic alcohols oxidations, the formation of benzaldehyde from benzyl alcohol (BOH2) exhibits a linear relation with time course. Furthermore, the oxidation of other benzylic show similar behaviour with lower reaction rate Fig. 5. Interestingly, the obtained results from aliphatic alcohols when compared to benzylic ones behave differently.

The tested aliphatic alcohols showed similar reaction rate but with slower reaction rate when compared to benzylic alcohol. This observation indicate that the substrate type has the effect on turnover rate with more reactive benzylic alcohols substrate the faster reaction rate, while with less reactive aliphatic substrates shows that catalyst oxidations contribution into the turnover rate only.

Catalytic reaction rates. The kinetic studies were investigated to establish an understanding of each reaction parameter rate for the oxidation of benzylic alcohol, particularly the ligand effect L2 and L4 were compared in each reaction component (see ESI†). The base effect NMI exhibited a first order dependence in both systems using L2 and L4 (Fig. 5a). Similarly, a first order reaction was also observed on TEMPO with non-zero

intercept (Fig. 5b). The Cu(OTf) loading amount reveals a varied-order dependence, with a second-order dependence at low [Cu] and a first-order dependence at high [Cu] using L2. However, applying L4 instead a L2 a first order dependence for [Cu] has been shown (Fig. 5c). The reaction rate of BOH has a first order dependence for oxygen pressure (Fig. 5d). A control experiments show that the first-order dependence on pO_2 does not arise from mass-transfer effects. For example, the rate continues to surge with increasing catalyst concentrations (see ESI†).

The data presented here provided a valuable insight into the roles of each component in the reaction system. The first order dependence on [O_2] and mixed second-order/first-order dependence [Cu] in L2 resembles reactions of O_2 with biomimetic nitrogen-chelated Cu^I complexes,[21,22,26,27] and the data is in consistence of the mechanism where O_2 is reacted with Cu^I to produce Cu^{II} superoxide species.[22,26]

The rate corresponding to a two-step sequence accounts for the second-order dependence on [Cu] at low [Cu], and first-order dependence at high [Cu]. However, a one sequence rate (first order) dependence on metal complex using L4 shows that the ligand type plays a key role in reaction rate. The ligand L4 weaker base than L2 that leads to a slower rate. Further studies will be needed to understand the origin of this difference. Noteworthy, the use of ancillary ligands it is tentatively attributed as base that should stabilize Cu^I–Cu^{II} oxo species. Table 2 summarise the reaction rate constant of all parameters control experiments show that oxidation of Cu^I to Cu^{II} by O_2 does not require TEMPOH. However, TEMPOH appears to be required to achieve a kinetically competent rate. At the start of the reaction, when no TEMPOH is available, we speculate that the substrate reacts with the peroxo complex species to afford Cu^{II}–OOH and Cu II– substrate species.[19–21]

We obtained the UV-Vis of Cu^IOTf/L4 to study the interaction between different components in the reaction mixture (Fig. 6), which is useful to learn more about unclear aspects from the kinetic approach. The metal-to-ligand charge-transfer MLCT sharp peaks was observed between 310 and 360 nm. This indicates that the replacement of coordinated solvent molecules is at the Cu^I site. Meanwhile the bubbling with O_2 through the solution shifted the band from 360 to 400 nm, which is attributed to dipolar interaction between the complex and the O_2 instead of the complex oxidation.[30] Broadening of the 400 nm band indicates a LMCT between NMI and the complex. New d–d transition band is formed at 510 nm after the NMI addition attributes to oxidation of the Cu^I to Cu^{II} species as postulated in other papers.[30] TEMPO addition gave similar bands between 410 and 510 nm. Therefore, we believe that the role of TEMPO is the activation and stabilization of O_2 in the active Cu^{II} species. Alcohol addition to the solution shows a disappearance of d–d band at 510, no broadening on band 410, and a negligible shift of the 410 band is observed.

Hammett studies. The use of Hammett correlation in such systems were used to detect the cationic species involvement in mechanism by C–H bond. Hammett studies were applied for various benzyl alcohols using independent rate measurement. Comparing the rates of various alcohols using L2 reveals a negligible electronic dependence Fig. 7. Noteworthy, if the kinetic selectivity was controlled by the H-atom abstraction step, a negative Hammett slop will be obtained. The Hammett slop in our case for both ligands are $\rho = +0.28$ and 0.33 respectively. The key step in the mechanism is not controlled by H-abstraction. As previously reported, this can be due to the preferential formation of the Cu^{II}–OCH_2R species derived from the more acidic alcohols.[20,21]

Substrates expansion for the catalytic system

After investigating the reaction mechanism, the alcohol substrates scope was examined using the catalytic system (L4) Table 3. The results showed that the system has an excellent applicability with no over oxidation by-product. It aerobically oxidizes benzylic type alcohols quantitatively with no significant effect of the substituent on the phenyl ring, either electron withdrawing or donating groups on the product yield.

Furthermore, the catalytic system showed good activity toward primary aliphatic alcohols oxidation with good yields. A moderate activity was observed for secondary alcohols such as

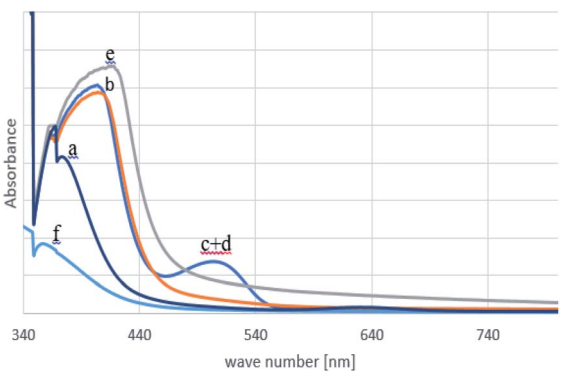

Fig. 6 Subsequent UV-Vis spectra of complex 0.01 mmol Cu^IOTf/L4 in acetonitrile solution (a) with L4, (b) after 20 min bubbling O_2 through this solution at 20 °C, (c) with NMI after 5 min, (d) with TEMPO immediately, (e) with BzOH immediately, and (f) BzOH 30 min.

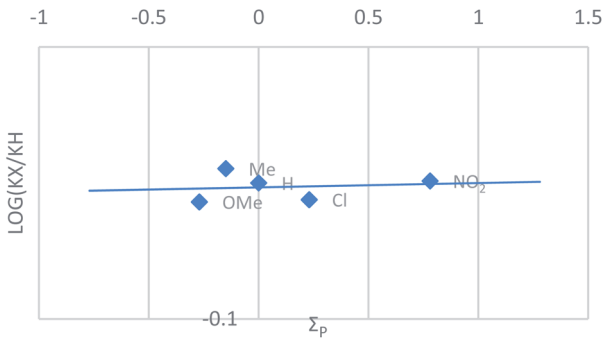

Fig. 7 Hammett plots reflecting a comparison of independent rate measurements of the *para* substituted $PhCH_2OH$ using L2. Standard reaction conditions: $PhCH_2OH$ (1 mmol, 130.2 mg), Cu(OTf) (0.05 mmol, 18.8 mg), L2 (0.05 mmol, 9.2 mg), TEMPO (0.05 mmol, 14.8 mg), air, 25 °C. Conversion calculated by GC analysis using 1,2-dichlorobenzene as internal standard.

Table 3 Substrate expansion for the tested catalytic system Cu/L2

Entry	Substrate	Product	Time [h]	Yield [%]
1			2	99
2	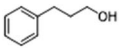	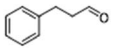	5	99
3	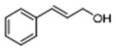	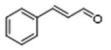	3	99
4	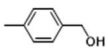	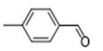	2	99
5	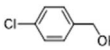	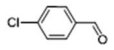	2	99
6	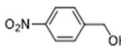	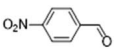	2	99
7	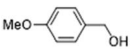	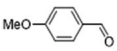	2	99
8			5	45
9			2	99
10			2	99
11			2	99
12	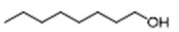		22	95
13	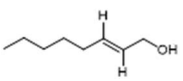	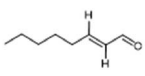	22	90
14	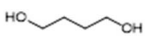	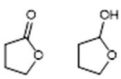	12	52, 30
15	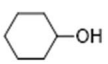		12	2

2-phenylethanol (entry 8), however, barely any activity to other secondary alcohol. It is noteworthy that the yield for the oxidation of cyclohexanol was negligible. This may be attributed to the volatile nature rather than poor catalytic efficiency.

In comparison of our results with previously reported Cu/TEMPO systems we found that the systems have shown a significantly preference to primary alcohols over secondary alcohols and successfully discriminate between the benzylic and aliphatic primary alcohols. The resutls were in consistance with previously reported Cu/TEMPO catalysts.[7–13] In oxidizing diols such 1,4-butandiol (entry 14), this system afforded the lactones in good yield comparable to Cu/ABNO.[31]

A simple model for oxidation reaction prediction – GAM

The simple model prediction was developed for the yield curves with a particular focus on predictors for L2 and L4 (Fig. S13–S19†). Using the results from a generalized additive model (GAM, including random effects), there is some evidence of a difference in yield curves between NMI 5 and 10 ($p = 0.0475$) (Fig. 8a) and also for alcohol (Aliph1 *versus* BOH1) ($p < 0.001$) but not for the other variables examined (see Fig. 8b). A significantly lower yield curve over most of the time period for the experiment is observed for BOH1 compared to Aliph1. A lower yield curve is observed for NMI 5 compared to NMI 10 only over the middle time period of the experiment. In terms of interaction with ligand type (L2 and L4) there appears to be some evidence of an interaction only between ligand type and alcohol over time ($p < 0.001$) and not for the other variables.

There is evidence of a different effect of alcohol on ligand type L2 compared to ligand type L4 with a significant effect of alcohol on L2 but not L4 (Fig. 9). This difference in effect could be due to a small number of experiments/yield curves over the entire time for L4 compared to L2. The result from the predictive model inconsistent with results we obtained from the kinetic studies. This shows the possibility to use such simple model to predict the results of multi variable component in the reaction with minimal statistically unnecessary screening reactions. We have to keep in mind the[32] necessity of large number of data to achieve a better understanding of all reaction components to reduce the level of uncertainty of the predictive model.

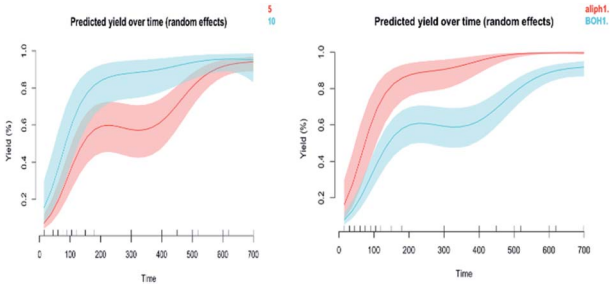

Fig. 8 (a) Predicted yield over time for NMI (5 and 10) using GAM results. (b) Predicted yield over time for alcohol (Aliph1 and BOH1) using GAM results.

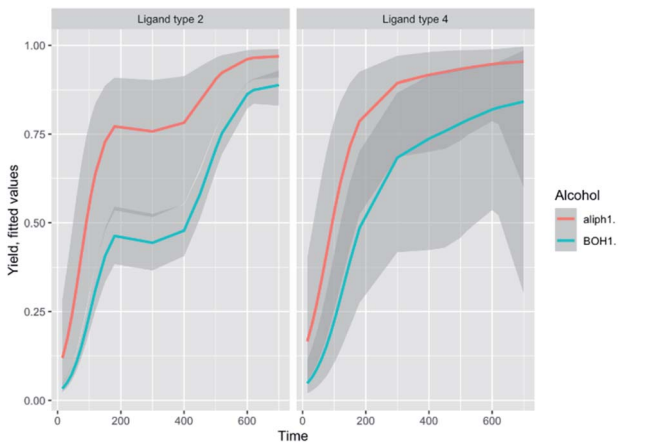

Fig. 9 Predicted yield over time for ligand type by alcohol (Aliph1 or BOH1).

Conclusion

The results provide insights into catalytic mechanism of furan ligand type in Cu/TEMPO/NMI that show a simple system can achieve the desired reactivity with ligand designing and benign reaction condition. The substitution of furan moity such L2 and L4 would change basicity of the ligand, thus increases the electron density of the metal centre; therefore, a higher oxidation reactivity is expected. Currently, the catalytic systems are aerobically oxidizing primary alcohols into aldehydes in excellent yields and selectivity. The kinetic studies shows that the base effect NMI exhibited a first order dependence in both systems using L2 and L4. Similarly, a first order reaction was also observed on TEMPO with non-zero intercept. The Cu(OTf) loading amount reveals a varied-order dependence, with a second-order dependence at low [Cu] and a first-order dependence at high [Cu] using L2. However, L4 showed a first order dependence for [Cu]. This variation of the rate comes from the difference in the basicity moity of ligand and consequently leads to a slower rate. The control experiments show that oxidation of Cu^{I} to Cu^{II} by O_2 does not require TEMPOH. However, TEMPOH appears to be required to achieve a kinetically competent rate. At the start of the reaction, when no TEMPOH is available, we speculate that the substrate reacts with the peroxo complex species to afford Cu^{II}–OOH and Cu^{II}–substrate species. The Hammett plot in our case oxidation reaction for both ligands L2 and L4 are $\rho = +0.28$ and 0.33 respectively. Therefore, the key step in the mechanism is not controlled by H-abstraction. The kinetic study in this work provides clear insight regarding the factors that play key role in reaction mechanism, which closely mimic galactose oxidase enzyme. The generalized additive model (GAM, including random effect) study allowed us to study simultaneously the four synthesis variables (reactant concentrations) and to map the nonlinear space. By means of clustering and factorial analysis of the multiparametric results, it was possible to correlate reaction composition with catalytic activity, ligand structure, and substrate behaviour. This hybrid system seems to be a useful tool in catalyst development through dimensional optimisation while reducing the screening of statistically poor active catalysis. This can be developed in the form a predictive model bearing in mind numerous numbers of reactions to be performed or to produce a massive dataset of this type of oxidation reactions. The predictive model will act as a useful tool towards understanding the key steps in the catalytic oxidation.

Author contributions

Conceptualization, A. A. H.; methodology, A. A. H., D. W.; validation, A. A. H. and D. W. T. R.; formal analysis, A. A. H.; investigation B. A., A. A. H.; resources, A. A. H.; data curation, A. A. H. and D. W.; writing—original draft preparation, A. A. H. and D. W. T. R.; writing—review and editing, A. A. H., D. W. and T. R.; visualization, A. A. H.; supervision, A. A. H.; project administration, A. A. H.; funding acquisition, A. A. H.

Conflicts of interest

There are no conflicts to declare.

Acknowledgements

This work was supported by the Deanship of Scientific Research at the University of Jordan.

Notes and references

1 M. Hudlicky, *Oxidations in Organic Chemistry*, American Chemical Society, Washington DC, 1990; Q. Cao, L. M. Dornan, L. Rogan, N. L. Hughes and M. J. Muldoon, *Chem. Commun.*, 2014, **50**, 4524; M. T. Räisänen, A. Al-Hunaiti, E. Atosuo, M. Kemell, M. Leskelä and T. Repo, *Catal. Sci. Technol.*, 2014, **4**, 2564–2573; A. Al-Hunaiti, Q. Mohaidat, I. Bsoul, S. Mahmood, D. Taher and T. Hussein, *Catalysts*, 2020, **10**, 839.
2 G. Tojo and M. I. Fernandez, *Oxidation of Alcohols to Aldehydes and Ketones*, Springer Verlag, New York, 2006.
3 G. Tojo and M. I. Fernandez, *Oxidation of Primary Alcohols to Carboxylic Acids*, Springer, New York, NY, 2007.
4 S. Caron, R. W. Dugger, S. G. Ruggeri, J. a Ragan and D. H. B. Ripin, *Chem. Rev.*, 2006, **106**, 2943.
5 D. J. C. Constable, P. J. Dunn, J. D. Hayler, G. R. Humphrey, J. L. Leazer Jr, R. J. Linderman, K. Lorenz, J. Manley, B. Pearlman, A. Wells, A. Zaks and T. Y. Zhang, *Green Chem.*, 2007, **9**, 411.
6 H. Liu, D. Ramella, P. Yu and Y. Luan, *RSC Adv.*, 2017, **7**, 22353.
7 R. Jlassi, A. P. C. Ribeiro, M. Mendes, W. Rekik, G. A. O. Tiago, K. T. Mahmudov, H. Naïli, M. F. C. Guedes da Silva and A. J. L. Pombeiro, *Polyhedron*, 2017, **129**, 182.
8 J. Rabeah, U. Bentrup, R. Stößer and A. Brückner, *Angew. Chem., Int. Ed.*, 2015, **127**, 11957.
9 S. E. Kesler and B. H. Wilkinson, *Geology*, 2008, **36**, 255–258.
10 G. R. Hemsworth, E. J. Taylor, R. Q. Kim, R. C. Gregory, S. J. Lewis, J. P. Turkenburg, A. Parkin, G. J. Davies and P. H. Walton, *J. Am. Chem. Soc.*, 2013, **135**, 6069.
11 R. A. Festa and D. J. Thiele, *Curr. Biol.*, 2011, **21**, R877.
12 R. R. Conry, Copper: inorganic & coordination chemistry based in part on the article copper: inorganic & coordination chemistry by Rebecca R. Conry & Kenneth D. Karlin which appeared in the encyclopedia of inorganic chemistry, *Encycl. Inorg. Chem*, John Wiley & Sons, Ltd, Chichester, UK, 1st edn, 2006.
13 M. M. Whittaker and J. W. Whittaker, *J. Biol. Chem.*, 1988, **263**, 6074; L. Marais and A. J. Swarts, *Catalysts*, 2019, **9**, 395; M. J. Muldoon, *Catal. Sci. Technol.*, 2014, **4**, 1720–1725.
14 P. J. Filial, A. Sibaouih, J. U. Ahmad, M. Nieger, M. T. Räisänen, M. Leskelä and T. Repo, *Adv. Synth. Catal.*, 2009, **351**, 2625.
15 E. Safaei, L. Hajikhanmirzaei, B. Karimi, A. Wojtczak, P. Cotič and Y.-I. Lee, *Polyhedron*, 2016, **106**, 153.
16 S. Adomeit, J. Rabeah, A. E. Surkus, U. Bentrup and A. Brückner, *Inorg. Chem.*, 2017, **56**, 684–691.

17 S. L. Zultanski, J. Zhao and S. S. Stahl, *J. Am. Chem. Soc.*, 2016, **138**, 6416.
18 J. M. Hoover, B. L. Ryland and S. S. Stahl, *J. Am. Chem. Soc.*, 2013, **135**, 2357.
19 J. E. Steves and S. S. Stahl, *J. Am. Chem. Soc.*, 2013, **135**, 15742.
20 S. S. Stahl, *J. Am. Chem. Soc.*, 2011, **133**, 16901.
21 P. Gamez, I. W. C. E. Arends, J. Reedijk and R. A. Sheldon, *Chem. Commun.*, 2003, 2414.
22 M. del Mar Conejo, J. Cantero, A. Pastor, E. Álvarez and A. Galindo, *Inorg. Chim. Acta*, 2018, **470**, 113–118.
23 W. Czepa, M. A. Fik, S. Witomska, M. Kubicki, G. Consiglio, P. Pawluć and V. Patroniak, *ChemistrySelect*, 2018, **3**, 9504–9509.
24 G. L. Tripodi, M. M. J. Dekker, J. Roithova and L. Que Jr, *Angew. Chem., Int. Ed.*, 2021, **60**, 7126–7131; *Angew. Chem.*, 2021, **133**, 7202–7207.
25 Z. Liu, Z. Shen, N. Zhang, W. Zhong and X. Liu, *Catal. Lett.*, 2018, **148**, 2709–2718; E. T. Kumpulainen and A. M. Koskinen, *Chem.–Eur. J.*, 2009, **15**, 10901–10911.
26 E. Lagerspets, K. Lagerblom, E. Heliövaara, O.-M. Hiltunen, K. Moslova, M. Nieger and T. Repo, *Mol. Catal.*, 2019, **468**, 75.
27 C. Feng, L. Cheng, H. Ma, L. Ma, Q. Wu and J. Yang, *Inorg. Chem.*, 2021, **60**, 14132–14141.
28 A. Ochen, R. Whitten, H. E. Aylott, K. Ruffell, G. D. Williams, F. Slater, A. Roberts, P. Evans, J. E. Steves and M. J. Sanganee, *Organometallics*, 2019, **38**, 176–184.
29 E. O. Nutting, K. Mao and S. S. Stahl, *J. Am. Chem. Soc.*, 2021, **143**, 10565–10570.
30 L. Marais, J. Bures, J. H. L. Jordaan, S. Mapolie and A. J. A. Swarts, *Org. Biomol. Chem.*, 2017, **15**, 6926–6933.
31 X. Xie and S. S. Stahl, *J. Am. Chem. Soc.*, 2015, **137**, 3767–3770; T. Y. Chen, Z. H. Wang, J. C. Xiao, Z. Cao, C. F. Yi and Z. H. Xu, *Asian J. Org. Chem.*, 2019, **8**, 1321–1324.
32 M. Holena and M. Baerns, *Catal. Today*, 2003, **81**, 485–494.